Oncogene (2011) 30, 4835–4842

www.nature.com/onc

SHORT COMMUNICATION

Hypoxia-driven cell motility reflects the interplay between JMY and HIF-1α

AS Coutts[1], IM Pires[2], L Weston[1], FM Buffa[3], M Milani[3], J-L Li[3], AL Harris[3], EM Hammond[2] and NB La Thangue[1]

[1]*Laboratory of Cancer Biology, Department of Oncology, University of Oxford, Oxford, Oxon, UK;* [2]*Department of Oncology, Cancer Research UK/MRC Gray Institute for Radiation Oncology and Biology, University of Oxford, Oxford, Oxon, UK and* [3]*Department of Oncology, Cancer Research UK/Molecular Oncology Laboratories, University of Oxford, Weatherall Institute of Molecular Medicine, Oxford, Oxon, UK*

Junction-mediating and regulatory protein (JMY) is a novel p53 cofactor that regulates p53 activity during stress. JMY interacts with p300/CBP, which are ubiquitous transcriptional co-activators that interact with a variety of sequence-specific transcription factors, including hypoxia-inducible factor-1α (HIF-1α). In addition, JMY is an actin-nucleating protein, which, through its WH2 domains, stimulates cell motility. In this study, we show that JMY is upregulated during hypoxia in a HIF-1α-dependent manner. The *JMY* gene contains HIF-responsive elements in its promoter region and HIF-1α is recruited to its promoter during hypoxia. HIF-1α drives transcription of *JMY*, which accounts for its induction under hypoxia. Moreover, the enhanced cell motility and invasion that occurs during hypoxia requires JMY, as depleting JMY under hypoxic conditions causes decreased cell motility. Our results establish the interplay between JMY and HIF-1α as a new mechanism that controls cell motility under hypoxic stress.
Oncogene (2011) **30,** 4835–4842; doi:10.1038/onc.2011.188; published online 30 May 2011

Keywords: JMY; HIF-1; actin; hypoxia; motility

JMY (junction-mediating and regulatory protein) was initially defined through studies on the p300/CBP family of transcriptional co-activators, which are ubiquitous transcriptional co-activators that interact with a variety of sequence-specific transcription factors, including p53. During the DNA damage response, JMY along with the p53 cofactors Strap and PRMT5 are brought together to influence p53 activity (Shikama *et al*., 1999; Demonacos *et al*., 2001; Jansson *et al*., 2008). The Mdm2 oncoprotein is a key regulator of the p53 response (Marine *et al*., 2006), and studies identified JMY as a new target through which Mdm2 regulates p53 activity (Coutts *et al*., 2007).

Correspondence: Dr NB La Thangue, Department of Oncology, University of Oxford, Old Road Campus Research Building, Old Road Campus, off Roosevelt Drive, Oxford, Oxon OX3 7DQ, UK.
E-mail: nick.lathangue@clinpharm.ox.ac.uk
Received 10 January 2011; revised 12 April 2011; accepted 13 April 2011; published online 30 May 2011

JMY contains three C-terminal WH2 (Wiskott–Aldrich syndrome protein (WASp)-homology 2) domains, which facilitate the assembly of actin monomers into newly formed actin filaments (Coutts *et al*., 2009; Zuchero *et al*., 2009). Through its ability to influence actin nucleation, JMY can enhance cell motility and invasion, which occurs, in part, through alterations in cadherin levels (Coutts *et al*., 2009). Moreover, during the DNA damage response, JMY becomes more nuclear, leading to enhanced p53 activity, whereas its effect on cell motility is diminished (Coutts *et al*., 2009). JMY is, thus, a dual-function protein, regulated, in part, through its subcellular localisation.

Hypoxia triggers an adaptive response and is an important physiological stress that is highly relevant to tumour progression. As tumours evolve, oxygen tension drops, which is associated with angiogenesis, tumour progression and metastasis (Harris, 2002). Oxygen homoeostasis is tightly regulated by the transcription factor hypoxia-inducible factor-1 (HIF-1), a heterodimeric complex composed of HIF-1α and HIF-1β (ARNT) (Wang *et al*., 1995). HIF-1α levels are kept low during normoxia, as HIF-1α is rapidly ubiquitinated and degraded by the 26S proteasome (Kaelin and Ratcliffe, 2008). During hypoxia, HIF-1α protein is stabilised and translocates to the nucleus where HIF-1 binds to hypoxia response elements (HREs) in target genes encoding proteins critical for many important cellular processes including angiogenesis, proliferation, apoptosis, glycolysis and invasion (Rankin and Giaccia, 2008; Semenza, 2010).

Many studies have demonstrated a significant correlation with hypoxia and metastasis (reviewed in Sullivan and Graham, 2007). In addition, HIF-1α regulates (both directly and indirectly) proteins that are key to metastatic potential, including, for example, E-cadherin, LOX and endothelin-1 (Erler *et al*., 2006; Krishnamachary *et al*., 2006; Spinella *et al*., 2007). In general, overexpression of HIF-1α in human tumours is often associated with poor prognosis and treatment failure, demonstrating the significance of this pathway in cancer biology (reviewed in (Semenza, 2010)).

As JMY is a stress-responsive protein involved in cell motility and invasion (Coutts *et al*., 2009; Zuchero *et al*., 2009), we wished to explore the role of JMY in the

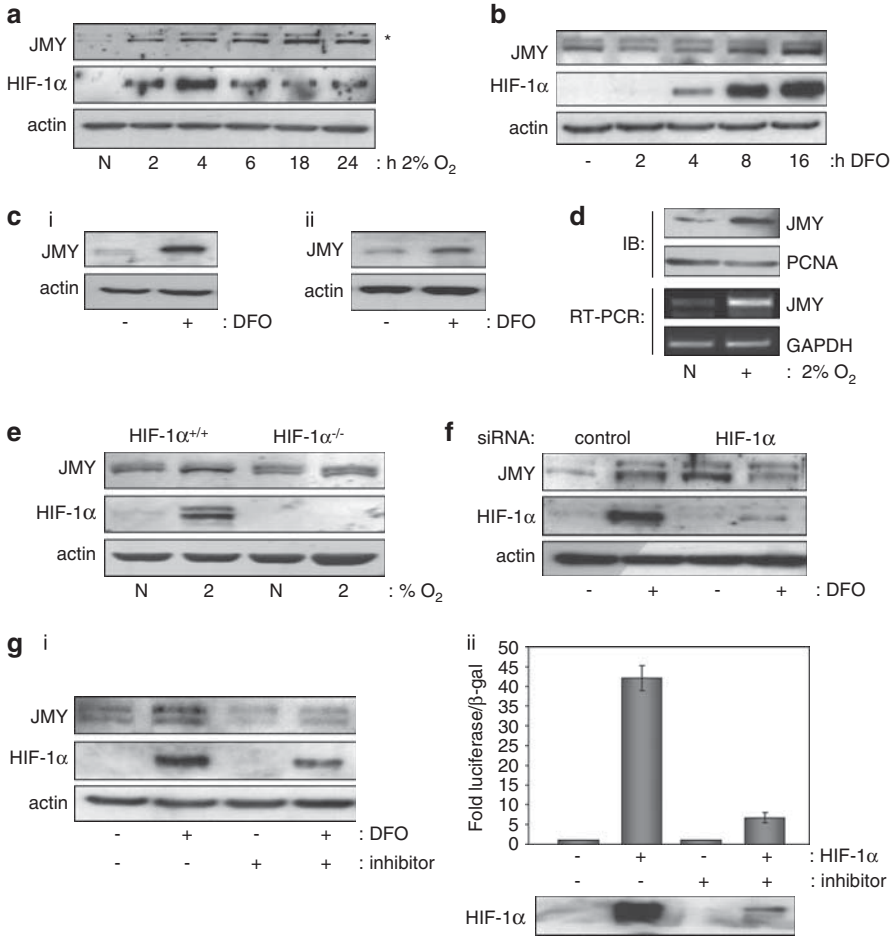

Figure 1 JMY is a hypoxia-responsive protein. (**a**) U2OS cells were incubated under normoxic (N) or hypoxic (2% O_2) conditions for the times indicated before harvesting. Endogenous JMY was detected using anti-JMY antibody L16 (Santa Cruz, Heidelberg, Germany). HIF-1α was detected using anti-HIF-1α antibody (BD Biosciences, Oxford, UK). Actin was detected using anti-actin antibody (Sigma-Aldrich, Dorset, UK). * Denotes nonspecific band (Coutts *et al*., 2009). (**b**) MCF-7 cells were treated with deferoxamine (DFO, 100 μM) for the time points indicated before harvesting. JMY and HIF-1α levels are shown. Actin was used as a loading control. (**c**) MCF-7 (**i**) or U2OS (**ii**) cells were treated with vehicle (−) or deferoxamine (+, DFO, 100 μM) for 16 h before harvesting. Cell extracts were run on SDS–PAGE and immunoblotted with anti-JMY antibody, and actin was used as a loading control. (**d**) MCF-7 cells were incubated under either normoxic (N) or hypoxic (+; 2% O_2) conditions for 16 h before harvesting. Cells were extracted for either protein for immunoblotting (IB) (upper two panels) or RNA (RT–PCR) (lower two panels). Blots were probed with anti-JMY antibody and PCNA (proliferating cell nuclear antigen) was used as a loading control. RT–PCR was performed on cDNA obtained from 1 μg of RNA from cells using Trizol reagent (Invitrogen, Paisley, UK) with JMY-specific primers (Forward 5′-gtagagcttttggacttg-3′; reverse 5′-tctgatctgctcgcatcc-3′) and GAPDH-specific primers were used as an input control. (**e**) HCT116 HIF-1α$^{+/+}$ (WT) or HIF-1α$^{-/-}$ were grown under normoxic (N) or hypoxic (2% O_2) conditions for 16 h before harvesting. Blots were probed with JMY and HIF-1α antibodies. Actin was used as a loading control. (**f**) MCF-7 cells were transfected with 25 nM of control (non-targeting control #2, Dharmacon/Thermo Scientific, Epsom, UK) or HIF-1α siRNA (Santa Cruz) using oligofectamine (Invitrogen). After 48 h, cells were treated with DFO (100 μM) and left for a further 24 h before harvesting. Blots were probed with JMY and HIF-1α antibodies. Actin was used as a loading control. (**g**) (**i**) MCF-7 cells were treated with vehicle (−) or DFO (+), 100 μM) with (+) or without (−) HIF-1α inhibitor (3-(2-(4-adamantan-1-yl-phenoxy)-acetylamino)-4-hydroxybenzoic acid methyl ester, Merck/Calbiochem, Nottingham, UK; inhibitor; 30 μM) for 16 h before harvesting. Blots were probed with JMY and HIF-1α antibodies, and actin was used as a loading control. (**ii**) Luciferase reporter assays were performed using U2OS cells as previously described (Chan *et al*., 2001). Cells were transfected, using GeneJuice (Merck), with 200 ng VEGF–luciferase construct (a kind gift from Peter Ratcliffe, University of Oxford) along with 400 ng empty vector (−) or HIF-1α expression vector (a kind gift from Shoumo Bhattacharya, University of Oxford) for 48 h before harvesting. Transfections also included 100 ng of pCMV-β-galactosidase (β-gal) plasmid as an internal control. Cells were treated as in (**i**) with HIF-1α inhibitor for 16 h before harvesting. Graph represents fold luciferase activity after normalising for β-gal, which was used as a measure of transfection efficiency. Blots underneath represent HIF-1α input levels.

cellular response to hypoxia. Our results indicate that JMY is upregulated during hypoxia and that its gene is a novel transcriptional target of HIF-1α. Hypoxia-responsive elements within the *JMY* proximal promoter are required for HIF-1α activation under hypoxic conditions. Significantly, JMY is required for cell motility and invasion during hypoxia, most likely mediated through its ability to foster actin nucleation. The interplay between JMY and HIF-1α thus defines a new pathway for regulating motility under hypoxic conditions.

We examined the levels of JMY in various cell types growing under hypoxic (2% O_2) conditions, and found that JMY was upregulated (Figure 1a, Supplementary Figure 1A). Moreover, the induction of JMY during

hypoxia occurred by 2 h, reflecting the induction of HIF-1α at a similar time point (Figure 1a). Additionally, JMY was upregulated after growth under a variety of oxygen concentrations, including anoxia (Supplementary Figures 1A and B), indicating JMY is sensitive to oxygen tensions ranging from mild (2–0.5%) to severe (<0.02%) hypoxia. Moreover, treating cells with deferoxamine (DFO), an iron chelator, which mimics certain properties of hypoxia by upregulating HIF-1α (Wang and Semenza, 1993), resulted in upregulation of JMY protein (Figures 1b and c i,ii), in a similar manner as HIF-1α (Figure 1b). Of note, JMY mRNA levels

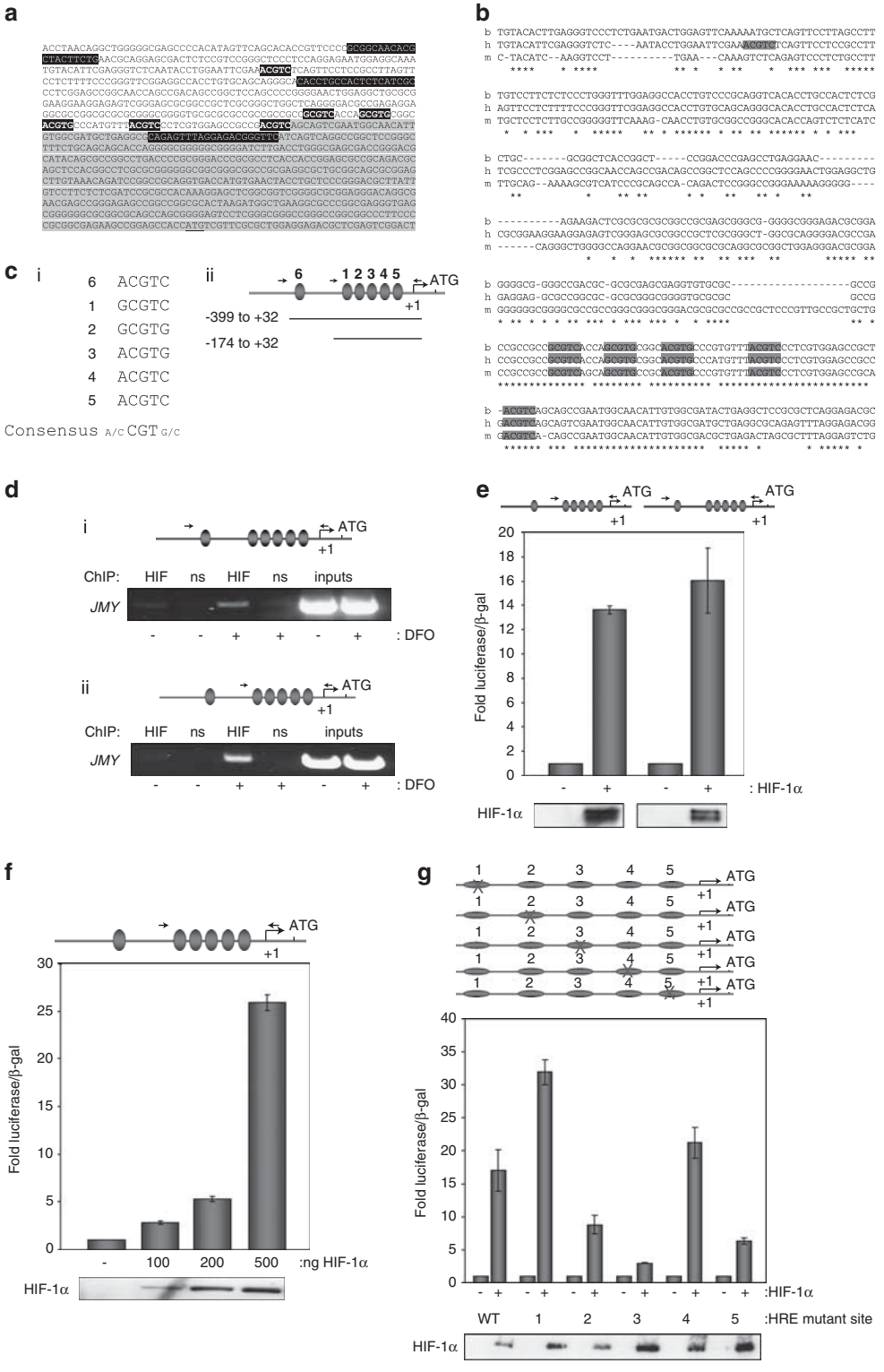

Figure 2 For caption see page 4838.

were induced along with JMY protein levels under hypoxia (Figure 1d). Together these data indicate that JMY is upregulated during hypoxia and further suggest that its transcriptional regulation is hypoxia-responsive.

As JMY is regulated at the transcriptional level during hypoxia and its regulation mimicked that seen with HIF-1α, we explored the possibility that HIF-1α might be involved in regulating JMY. Initially, we examined JMY levels during hypoxia in HCT116 cells that are HIF-1α$^{-/-}$ (Dang *et al*., 2006) compared with normal counterparts, HIF-1α$^{+/+}$. Interestingly, JMY was not upregulated during hypoxia in HCT116 HIF-1α$^{-/-}$ cells, but was in the parental, HIF-1α$^{+/+}$, cells (Figure 1e). This suggested that JMY upregulation during hypoxia relies on HIF-1α. To confirm this, using another cell system, MCF-7 cells were depleted of HIF-1α by siRNA treatment and JMY levels examined during hypoxic conditions. Indeed, depletion of HIF-1α under DFO treatment prevented upregulation of JMY (Figure 1f). To provide further evidence that JMY upregulation relies on HIF-1α activity, cells were treated with a HIF-1α inhibitor (3-(2-(4-adamantan-1-yl-phenoxy)-acetylamino)-4-hydroxybenzoic acid methyl ester), which prevents HIF-1α transcriptional activity and reduces HIF-1α protein levels (Lee *et al*., 2007; Figure 1gii). Treating cells with DFO resulted in an upregulation of both JMY and HIF-1α (Figure 1gi), whereas co-treatment with the HIF-1α inhibitor reduced the upregulation of both JMY and HIF-1α (Figure 1gi). Together these data confirm that JMY requires HIF-1α activity for upregulation during hypoxia.

Inspection of the upstream promoter region of JMY identified several putative HRE that closely resembled the canonical sequence A/G CGTG as well as a broader, though less well-defined, sequence BACGTSSK (B = T/G/C; S = G/C; K = T/G (Rankin and Giaccia, 2008; Semenza, 2010)), in the proximal *JMY* promoter (Figure 2a). Interestingly, six putative HREs were identified in the human *JMY* promoter (Figures 2a and ci). Of these, the cluster of five is highly conserved across different species, whereas a more distal HRE is only found in the human *JMY* promoter (Figure 2b). Primers were designed to encompass this region for use in chromatin immunoprecipitation (Figure 2a) to explore the recruitment of HIF-1α to the *JMY* promoter. Indeed, HIF-1α was recruited to the *JMY* promoter under DFO treatment (Figure 2d i,ii), supporting the existence of functional HREs in this region.

To further study the regulation of this region by HIF-1α, the *JMY* promoter (−399 to +32, encompassing all six HREs and −174 to +32, encompassing five proximal HREs) was cloned into pGL3-basic in order to perform luciferase assays (Figure 2cii). HIF-1α activated both reporter constructs (Figure 2e), confirming the ability of HIF-1α to regulate *JMY* expression. Additionally, HIF-1α regulation of the *JMY* promoter occurred in a dose-responsive manner (Figure 2f). To establish the functional significance of HIF-1α in regulating JMY transcription, the five highly conserved individual HREs (1–5; Figure 2cii) were each mutated and the ability of HIF-1α to transcriptionally activate the mutated *JMY* promoter constructs was assessed in luciferase assays. Mutating the five HREs resulted in near complete ablation of HIF-1α activation of the *JMY* promoter (Supplementary Figure 1C). Interestingly, mutating HRE-1 and -4 consistently resulted in enhanced activation of the *JMY* promoter by HIF-1α (Figure 2g). Mutating HRE-3 had the most consistent effect in terms of reducing HIF-1α activation of the *JMY* promoter, whereas loss of HRE-2 and -5 also resulted in inhibition of HIF-1α activity (Figure 2g). Together these data show that *JMY* is a HIF-1α responsive gene and defines the mechanism involved.

Figure 2 JMY promoter is HIF-1α-responsive element. (**a**) Sequence of the human JMY 5′ promoter region. Grey shading indicates exon 1. Underlined ATG is initiating methionine. Blue shading indicates primers used for chromatin immunoprecipitation (ChIP) analysis. The putative HREs are shaded in red. (**b**) Line-up shows the conservation of the JMY promoter around the HREs. m, mouse, h, human, b, bull. Red shading indicates HREs. (**c**) (**i**) Comparison of JMY HREs to consensus. (**ii**) Schematic represents the two regions of the JMY promoter cloned into pGL3-basic for reporter assays. Base pair numbering is relative to the transcription start site. Grey-shaded ovals represent individual HREs and numbers 1–5 represent the individual HREs mutated in (**g**). (**d**) Chromatin immunoprecipitation was performed on chromatin from MCF-7 cells treated with either vehicle (−) or 100 μM deferoxamine (DFO, +) for 16 h as previously described (Zalmas *et al*., 2008). HIF-1α was immunoprecipitated with anti-HIF-1α antibody (HIF). ns, nonspecific control IgG immunoprecipitation. Inputs represent non-immunoprecipitated chromatin. Immunoprecipitated chromatin was purified using Qiaquick PCR purification kit (Qiagen, Crawley, UK) according to the manufacturer's instructions. PCR was performed on chromatin using JMY-specific primers (JMYCHIPF1 5′-gcggcaacacgctacttct-3′; JMYCHIPF2 5′-cacctgccactctcatcgc-3′; JMYCHIPR2 5′-gaacccgtctcctaaactctg-3′). (**i**) PCR, on chromatin, performed with primers encompassing six HREs (JMYCHIPF1/JMYCHIPR2). (**ii**) PCR, on chromatin, performed with primers encompassing five HREs (JMYCHIPF2/JMYCHIPR2). (**e**) Luciferase reporter assays were performed using U2OS cells as previously described (Chan *et al*., 2001). Cells were transfected with 100 ng JMY promoter luciferase constructs, as denoted along either with 400 ng empty vector (−) or with HIF-1α expression vector (+) for 48 h before harvesting. Graph represents fold luciferase activity after normalising for β-galactosidase (β-gal), which was used as a measure of transfection efficiency. Blots underneath represent HIF-1α input levels. (**f**) Luciferase reporter assays were performed using U2OS cells. Cells were transfected with 100 ng JMY promoter luciferase construct −174 to +32, along either with empty vector (−) or with the appropriate amount of HIF-1α expression vector (+), as denoted. Graph represents fold luciferase activity after normalising for β-gal, which was used as a measure of transfection efficiency. Blot underneath represents HIF-1α input levels. (**g**) Luciferase reporter assays were performed using U2OS cells transfected with 100 ng JMY promoter luciferase construct −174 to +32, along either with 400 ng empty vector (−) or with HIF-1α expression vector (+) for 48 h before harvesting. Graph represents fold luciferase activity after normalising for β-gal, which was used as a measure of transfection efficiency. WT, wild-type JMY promoter −174 to +32, 1–5 denotes the HRE that was mutated (see (**cii**). HREs 1–5 (see **c**)) were mutated to AAAAA using QuickChange Site-directed mutagenesis kit (Agilent Technologies, Stockport, UK) according to the manufacturer's instructions. Blot underneath represents HIF-1α input levels. A full colour version of this figure is available at the *Oncogene* journal online.

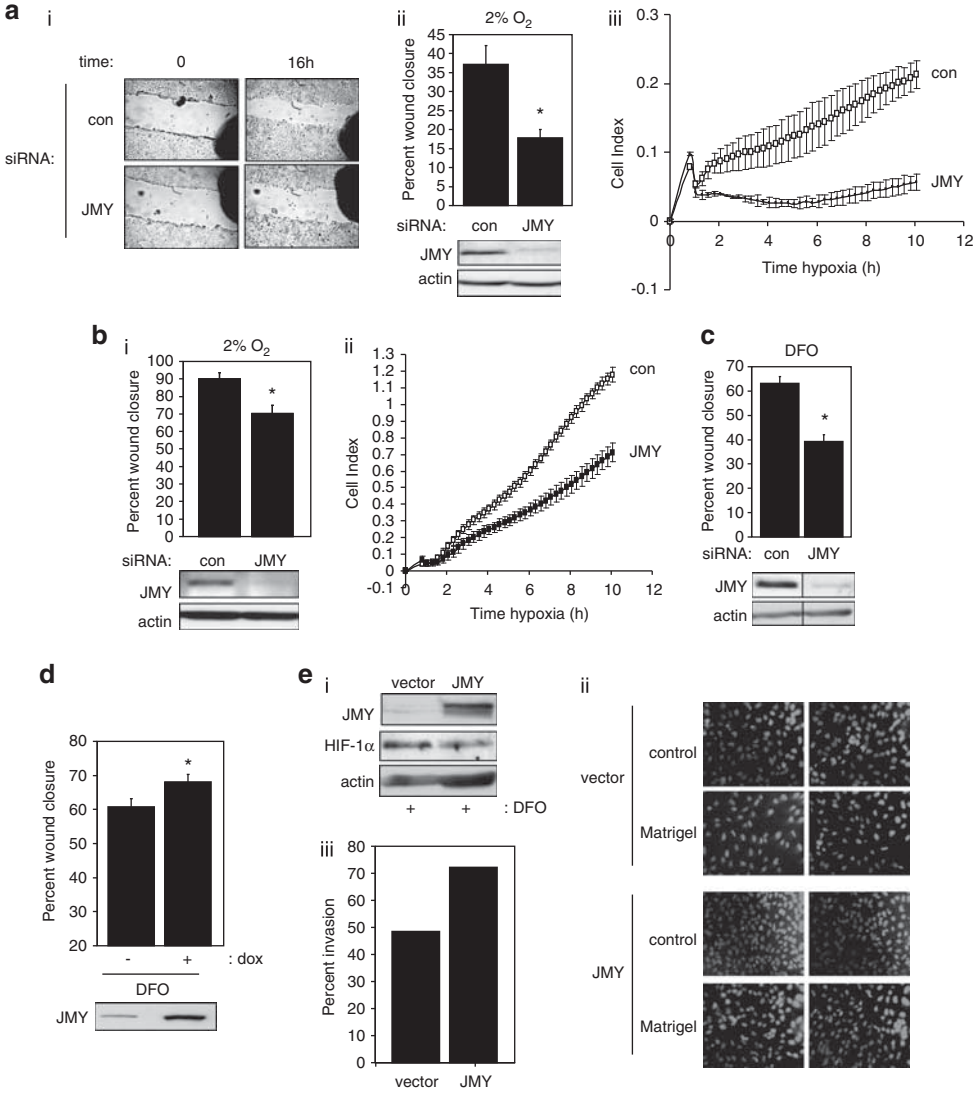

Figure 3 JMY influences motility during hypoxia. (**a**) (**i**) MCF-7 cells were treated with 25 nM non-targetting (con) or JMY siRNA (Coutts *et al*., 2009) for 72 h before performing scratch wound assays. Scratch wound assays were performed on confluent cells as previously described (Coutts *et al*., 2009). Photographs were taken immediately after wounding (time 0), and after 16 h incubation under 2% O_2. Graph in (**ii**) represents percentage wound closure after 16 h. Values represent mean ± s.e.m., $^*P<0.001$, Student's *t*-test, $n=3$ independent experiments. Blots underneath represent the degree of JMY knockdown. (**iii**) MCF-7 cells were treated as in (**i**) for 72 h. Cells were re-plated into CIM-plate 16 (Roche Diagnostics, GmbH, Germany) with 8 μm pores. These specially designed 'transwells' measure capacitance on the underside of the dividing membrane (RTCA DP instrument, Roche Diagnostics). In total, 40 000 cells in serum-free media were seeded into the upper chamber, and the lower chamber contained 10% FBS-DMEM as a chemoattractant. Experiments were carried out using the RTCA DP instrument (Roche Diagnostics), which was placed in a humidified incubator maintained at 37 °C with 3% O_2/5% CO_2. The electronic sensors provided a continuous and quantitative measurement of the cell index (reflecting impedence, which depends on the number of attached cells; for example, lower cell index reflects that less cells migrated) in each well. The CIM-plate 16 was monitored every 15 min for 10 h. (**b**) (**i**) MDA-MB-231 cells were treated as in (**a**) and scratch wound assays were performed. Graph represents percentage wound closure after 16 h. Values represent mean ± s.e.m., $^*P<0.005$, Student's *t*-test, $n=2$ independent experiments. Blots underneath represent the degree of JMY knockdown. (**ii**) Cells were treated as in (**i**) before performing migration assays as outlined in (**aiii**). (**c**) HEK 293 cells were treated with control (con) or JMY siRNA for 72 h before performing scratch wound assays followed by treating cells for an additional 16 h with 100 μM deferoxamine (DFO). Graph represents percentage wound closure after 16 h. Values represent mean ± s.e.m., $^*P<0.001$, Student's *t*-test, $n=2$ independent experiments. Blots underneath represent the degree of JMY knockdown. (**d**) Inducible stable JMY overexpressing U2OS cells (Coutts *et al*., 2009) treated with vehicle control (−) or doxycycline (+, dox, 100 μg/ml) along with 100 μM deferoxamine (DFO) at the time of performing scratch wound assays. Graph represents percentage wound closure after 16 h. Values represent mean ± s.e.m., $^*P<0.05$, Student's *t*-test, $n=2$ independent experiments. Blot underneath represents inducible JMY levels. (**e**) (**i**) U2OS stable-inducible JMY cells (JMY) or an empty vector control cell line (vector) (Coutts *et al*., 2009) were treated with 100 μM deferoxamine (DFO) for 22 h along with doxycycline (1 μg/ml). Blots were probed with anti-JMY and anti-HIF-1α antibodies, and actin was used as a loading control. (**ii**) In total, 1×10^5 U2OS stable-inducible wild-type JMY cells (JMY) or empty vector control cells (vector), treated as in (**i**), were plated on both control and Matrigel chambers and treated with 100 μM DFO. Matrigel chamber cell migration assays were performed using Matrigel Invasion Chambers (BD Biosciences) with an 8 μm pore size according to the manufacturer's protocol. Cells were allowed to invade for 22 h before fixing and staining with propidium iodide to visualise nuclei. Results are representative of two individual experiments. Graph in (**iii**) represents percentage of cells invaded with DFO treatment. A full colour version of this figure is available at the *Oncogene* journal online.

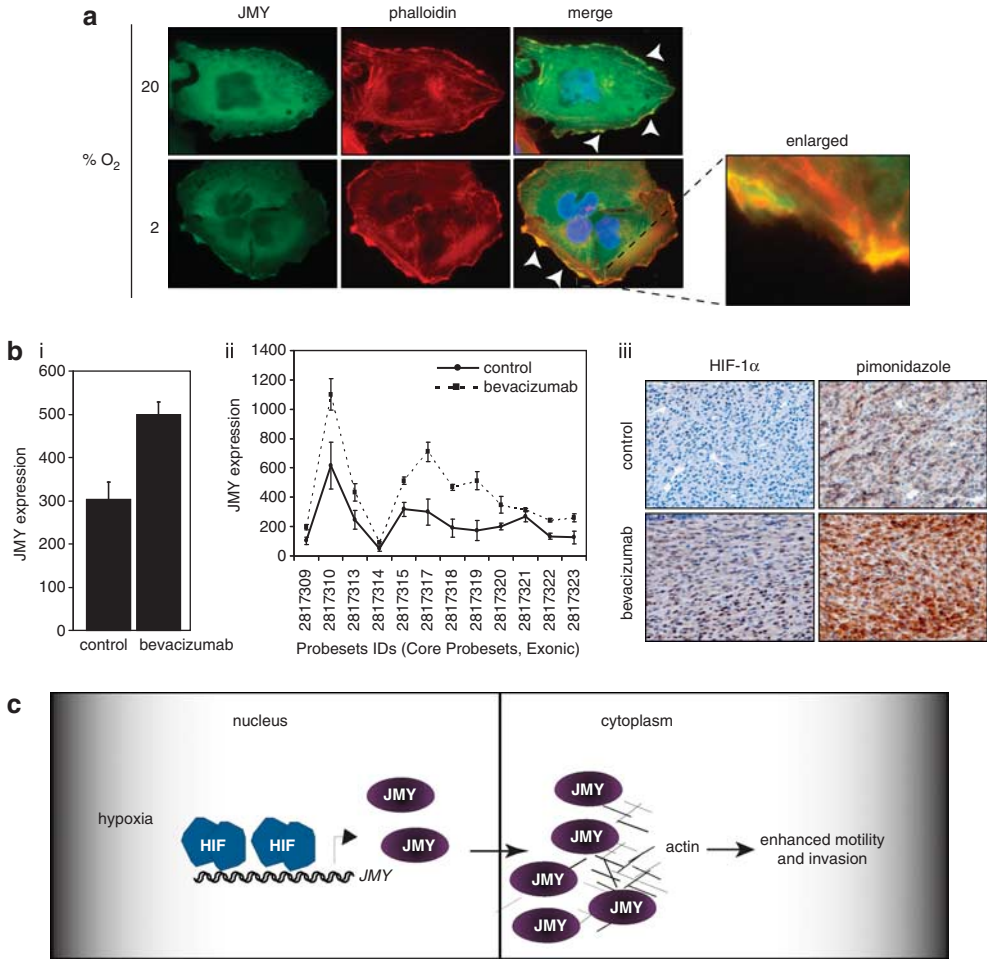

Figure 4 JMY localises with actin during hypoxia. (**a**) U2OS cells were plated onto 13 mm coverslips and transfected with HA-JMY (Coutts *et al*., 2009). 24 h later, coverslips were grown under the oxygen concentrations denoted for 16 h before fixing and processing for immunofluorescence. Immunofluorescence was performed as previously described (Coutts *et al*., 2009). JMY was detected with anti-HA antibody HA11 (Covance, Leeds, UK) and phalloidin was used to stain F-actin. DAPI (4′6′-diamidino-2-phenylindole) was used to visualise nuclei. The arrowheads indicate regions of JMY and actin colocalisation. Enlarged region shows JMY and actin colocalisation under hypoxia. (**b**) Triplicate experiments in (**i**) U87 and (**ii**) MDA-MB-231 xenografts comparing three controls with three bevacizumab (anti-VEGF mAb) tumours. JMY expression was measured by Affymetrix Plus2 arrays (Affymetrix, High Wycombe, UK) in (**i**) and Affymetrix Human Exon 1 ST arrays in (**ii**). Data were RMA processed, quantile normalised and logged base2. Plus2 arrays: graph represents mean ± s.e.m., $P = 0.028$, Student's *t*-test. Exon arrays: graph represents mean ± s.e.m., for each exonic probe set. Analysis of variance was performed including treatment (bevacizumab versus control) as factor and probe set as random effect. $F = 79.3$, $P = 2.E\text{-}6$. Only core exonic probe sets are shown. Xenografts: all protocols were carried out under the Home Office regulations (Li *et al*., 2007). The tumour cells (10^7) were implanted into 6- to 8-week-old female BALB/c SCID mice (Harlan Sprague–Dawley, Inc., Indianapolis, IN, USA) s.c. with 50 μl of cell suspension with an equal volume of Matrigel (BD Bioscience). Each group consisted of five mice. Tumour growth was monitored and measured using calipers. Tumour volume was calculated from a formula ($V = L \times W \times H \times 0.52$). Bevacizumab was injected i.p. every 3 days at a dose of 10 mg/kg, starting when the tumour reached 150 mm^3. Tumour samples were collected at the end of experiments and were freshly frozen in liquid N_2. RNA extraction from the tumour samples was performed as described previously (Li *et al*., 2007). Microarray analyses were carried out at the CRUK microarray services centre in Manchester. (**iii**) Immunostaining on tumour sections from U87 xenografts treated as described above. Tumour-bearing mice were injected i.v. with 2 mg pimonidazole (Hypoxylprobe-1) in 0.9% saline at 30 min before killing of the mouse (Li *et al*., 2007) and staining for pimonidazole was performed using the Hypoxyprobe-1 kit (Chemicon, Millipore, Watford, UK) according to the manufacturer's instructions. HIF-1α staining was performed as previously described (Biswas *et al*., 2010). (**c**) Model depicts function of JMY during hypoxia. In hypoxic conditions, JMY levels are enhanced through HIF-1-dependent transcriptional activation of JMY. JMY influences the motility and invasion through its ability to nucleate cytoplasmic actin.

We explored the role of JMY in cell motility during hypoxia. When JMY was depleted (through treatment with siRNA) from MCF-7 human breast cancer cells, there was a marked decrease in their ability to migrate into newly formed wounds (Figure 3ai). Although the control siRNA-treated cells showed an approximately 37% closure after 24 h, the JMY siRNA-treated cells showed only an approximately 17% closure after 24 h (Figure 3aii). Similar results were also observed with a variety of other cell types, including MDA-MB-231 and HEK 293 (Figure 3b and Supplementary Figure 2A). To gain further support, cell migration was measured in real-time where depletion of endogenous JMY resulted in decreased migration kinetics (Figures

3aiii and bii). Importantly, the kinetic analysis demonstrated that JMY depletion inhibits migration as early as 2 h (Figures 3aiii and bii), which thus rules out the influence of proliferation on cell motility.

Additionally, under DFO treatment, JMY-depleted cells showed a significant decrease in their ability to migrate into newly formed wounds (Figure 3c). Consistent with this observation, overexpression of JMY under DFO treatment augmented cell motility (Figure 3d). Real-time measurement of cell migration demonstrated that at early time points the induction of ectopic JMY resulted in a significant enhancement of migration during hypoxia (Supplementary Figure 2B). Moreover, ectopic JMY (Figure 3ei) augmented invasion through Matrigel (Figure 3e ii, iii). Together these data demonstrate that JMY is necessary for hyoxia-regulated cell motility.

The ability of JMY to influence cell motility during the DNA damage response is, in part, regulated by its localisation (Coutts *et al*., 2009). Thus, we wished to examine the localisation of JMY during hypoxia. In unperturbed normoxic cells (20% O_2) JMY was present in the cytoplasm, where it localised with actin (Figure 4a). During hypoxia, JMY was also able to colocalise with actin at the cell periphery, and similar to normoxic conditions, JMY remained primarily cytoplasmic (Figure 4a and Supplementary Figure 3). Thus, the presence of JMY at actin-containing structures under hypoxic conditions is consistent with its role in regulating cell motility (Figure 4b).

To explore the *in vivo* regulation of JMY, we examined JMY levels in xenografts from bevacizumab (anti-VEGF)-treated tumours, which increases intratumoral hypoxia (Ferrara *et al*., 2005; Rapisarda *et al*., 2009). Importantly, this correlated with a significant upregulation of *JMY* (Figure 4b i,ii). As anticipated, elevated HIF-1α levels and intratumoral hypoxia, as assessed by anti-HIF-1α and pimonidazole staining, were apparent (Figure 4biii). Thus, these data demonstrate that in hypoxic tumours *in vivo* JMY expression coincides with increased HIF-1α activity.

Our study demonstrates an important and novel link between the actin-nucleating factor JMY and HIF-1α. JMY is a novel *HIF-1α* target gene that mediates cell motility and invasion during hypoxia (Figure 4c). The ability of HIF-1α to activate JMY under hypoxic conditions provides a mechanism that maintains JMY at sufficient concentrations in hypoxic cells to facilitate cell motility. Given the enhanced cell motility that occurs under hypoxia (Sullivan and Graham, 2007), it makes sense that actin nucleation factors that augment cell motility, like JMY, should be responsive to such stimuli. Importantly, this study defines another pathway through which hypoxia and the DNA damage response can be integrated and suggests that JMY may be a clinically relevant target during tumour progression.

Conflict of interest

The authors declare no conflict of interest.

Acknowledgements

We thank the MRC, CRUK, LRF and AICR for support. ASC and LW are funded by MRC and CRUK (grant # C300/6731). IMP and EMH are funded by CRUK (grant # C6415/A9321). We also thank Long Dang, Peter Ratcliffe and Shoumo Bhattacharya for providing invaluable reagents.

References

Biswas S, Troy H, Leek R, Chung YL, Li JL, Raval RR *et al*. (2010). Effects of HIF-1alpha and HIF-2alpha on growth and metabolism of clear-cell renal cell carcinoma 786-0 xenografts. *J Oncol* **2010**: 757908.

Chan HM, Krstic-Demonacos M, Smith L, Demonacos C, La Thangue NB. (2001). Acetylation control of the retinoblastoma tumour-suppressor protein. *Nat Cell Biol* **3**: 667–674.

Coutts AS, Boulahbel H, Graham A, La Thangue NB. (2007). Mdm2 targets the p53 transcription cofactor JMY for degradation. *EMBO Rep* **8**: 84–90.

Coutts AS, Weston L, La Thangue NB. (2009). A transcription co-factor integrates cell adhesion and motility with the p53 response. *Proc Natl Acad Sci USA* **106**: 19872–19877.

Dang DT, Chen F, Gardner LB, Cummins JM, Rago C, Bunz F *et al*. (2006). Hypoxia-inducible factor-1alpha promotes nonhypoxia-mediated proliferation in colon cancer cells and xenografts. *Cancer Res* **66**: 1684–1936.

Demonacos C, Krstic-Demonacos M, La Thangue NB. (2001). A TPR motif cofactor contributes to p300 activity in the p53 response. *Mol Cell* **8**: 71–84.

Erler JT, Bennewith KL, Nicolau M, Dornhofer N, Kong C, Le QT *et al*. (2006). Lysyl oxidase is essential for hypoxia-induced metastasis. *Nature* **440**: 1222–1226.

Ferrara N, Hillan KJ, Novotny W. (2005). Bevacizumab (Avastin), a humanized anti-VEGF monoclonal antibody for cancer therapy. *Biochem Biophys Res Commun* **333**: 328–335.

Harris AL. (2002). Hypoxia–a key regulatory factor in tumour growth. *Nat Rev Cancer* **2**: 38–47.

Jansson M, Durant ST, Cho EC, Sheahan S, Edelmann M, Kessler B *et al*. (2008). Arginine methylation regulates the p53 response. *Nat Cell Biol* **10**: 1431–1439.

Kaelin Jr WG, Ratcliffe PJ. (2008). Oxygen sensing by metazoans: the central role of the HIF hydroxylase pathway. *Mol Cell* **30**: 393–402.

Krishnamachary B, Zagzag D, Nagasawa H, Rainey K, Okuyama H, Baek JH *et al*. (2006). Hypoxia-inducible factor-1-dependent repression of E-cadherin in von Hippel-Lindau tumor suppressor-null renal cell carcinoma mediated by TCF3, ZFHX1A, and ZFHX1B. *Cancer Res* **66**: 2725–2731.

Lee K, Lee JH, Boovanahalli SK, Jin Y, Lee M, Jin X *et al*. (2007). (Aryloxyacetylamino)benzoic acid analogues: a new class of hypoxia-inducible factor-1 inhibitors. *J Med Chem* **50**: 1675–1684.

Li JL, Sainson RC, Shi W, Leek R, Harrington LS, Preusser M *et al*. (2007). Delta-like 4 Notch ligand regulates tumor angiogenesis, improves tumor vascular function, and promotes tumor growth *in vivo*. *Cancer Res* **67**: 11244–11253.

Marine JC, Francoz S, Maetens M, Wahl G, Toledo F, Lozano G. (2006). Keeping p53 in check: essential and synergistic functions of Mdm2 and Mdm4. *Cell Death Differ* **13**: 927–934.

Rankin EB, Giaccia AJ. (2008). The role of hypoxia-inducible factors in tumorigenesis. *Cell Death Differ* **15**: 678–685.

Rapisarda A, Shoemaker RH, Melillo G. (2009). Antiangiogenic agents and HIF-1 inhibitors meet at the crossroads. *Cell Cycle* **8**: 4040–4043.

Semenza GL. (2010). Defining the role of hypoxia-inducible factor 1 in cancer biology and therapeutics. *Oncogene* **29**: 625–634.

Shikama N, Lee CW, France S, Delavaine L, Lyon J, Krstic-Demonacos M *et al*. (1999). A novel cofactor for p300 that regulates the p53 response. *Mol Cell* **4**: 365–376.

Spinella F, Rosano L, Di Castro V, Decandia S, Nicotra MR, Natali PG *et al*. (2007). Endothelin-1 and endothelin-3 promote invasive behavior via hypoxia-inducible factor-1alpha in human melanoma cells. *Cancer Res* **67**: 1725–1734.

Sullivan R, Graham CH. (2007). Hypoxia-driven selection of the metastatic phenotype. *Cancer Metastasis Rev* **26**: 319–331.

Wang GL, Jiang BH, Rue EA, Semenza GL. (1995). Hypoxia-inducible factor 1 is a basic-helix-loop-helix-PAS heterodimer regulated by cellular O_2 tension. *Proc Natl Acad Sci USA* **92**: 5510–5514.

Wang GL, Semenza GL. (1993). Desferrioxamine induces erythropoietin gene expression and hypoxia-inducible factor 1 DNA-binding activity: implications for models of hypoxia signal transduction. *Blood* **82**: 3610–3615.

Zalmas LP, Zhao X, Graham AL, Fisher R, Reilly C, Coutts AS *et al*. (2008). DNA-damage response control of E2F7 and E2F8. *EMBO Rep* **9**: 252–259.

Zuchero JB, Coutts AS, Quinlan ME, La Thangue NB, Mullins RD. (2009). p53-cofactor JMY is a multifunctional actin nucleation factor. *Nat Cell Biol* **11**: 451–459.

Supplementary Information accompanies the paper on the Oncogene website (http://www.nature.com/onc)